# **CHAPTER 32**

## THE FLUID MECHANICS OF WAVES APPROACHING BREAKING

#### by

D. H. Peregrine<sup>1</sup> E. D. Cokelet<sup>2</sup>

P. McIver<sup>3</sup>

#### Abstract

Numerical computations of water waves deforming until an overhanging, incipient jet has formed near the crest are studied in detail. Velocity and acceleration plots lead to the identification of three regions in the water which appear to be significant in the approach to breaking. In particular there is a region with particle accelerations greater than the acceleration of gravity.

# 1. Introduction

The initial stages of a plunging breaker are described from calculations by Longuet-Higgins and Cokelet (1976). They succeeded in computing the motion of particles on the surface of deep-water waves which are periodic in space. Similar computations are the basis of the present work which considers the flow properties in more detail.

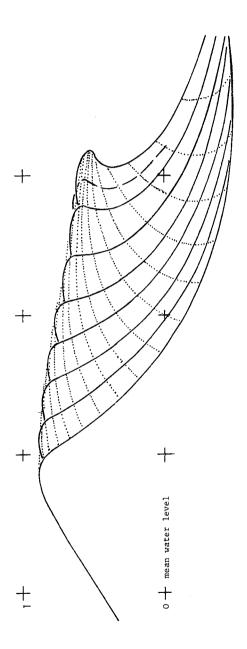
The mathematical model is for irrotational flow. The viscosity, the surface tension and the density of the fluid above the free surface are all taken to be zero. The only physical quantities which are present in the flow are the fluid's inertia and gravity. This appears to be quite sufficient since realistic looking results are obtained up to a time when a portion of the surface near the wave crest has been projected forward as an overhanging incipient jet. The numerical scheme then loses accuracy rapidly, apparently because the surface curvature has become too large for the method to resolve without more points along the wave profile.

Waves can be forced to break in several different ways. For these deep-water waves Longuet-Higgins and Cokelet (1978) describe how a small growing, normal-mode perturbation grows until waves break, and Cokelet (1979) shows how sinusoidal waves of sufficient initial amplitude also break, even if their energy density is less than that of the highest wave. Longuet-Higgins and Cokelet (1976) used a pressure distribution

<sup>&</sup>lt;sup>1</sup>Reader in Mathematics, University of Bristol, England

<sup>&</sup>lt;sup>2</sup>Oceanographer, Pacific Marine Environmental Laboratory/NOAA, Seattle, Washington, U.S.A.

<sup>&</sup>lt;sup>3</sup>Research Assistant, University of Bristol, England





imposed on the free surface for a limited time to drive the waves to break, and the same set of solutions are considered in more detail here. Full details of the method are to be found in that paper.

Details relevant to this work include the units used and the particular initial and forcing conditions. Units are made dimensionless using the fluid density, the acceleration due to gravity and the wave number of the waves. That means the waves have wavelength,  $L = 2\pi$ , and the phase velocity and radian frequency of infinitesimal waves of that wavelength are equal to one. The infinitesimal wave period is  $2\pi$ . The initial conditions are an accurate, steadily-progressing wave of steepness H/L = 0.13, or ak = 0.40, which may be compared with the values 0.14, or 0.43, for the steepest wave.

The wave forcing is by a sinusoidal pressure pattern travelling at the same speed as the initial wave, in quadrature with the wave profile to give an energy growth and smoothly applied for o < t <  $\pi$ . The value,  $p_0$ , of the maximum pressure used is a useful parameter for identifying particular cases.

## 2. Surface Profiles and the Flow Field

Some profiles of the surface for p = 0.0729, 0.100, 0.126 and 0.146 are given by Longuet-Higgins and Cokelet (1976). A sequence of profiles for p = 0.200 are shown in Figure 1. This figure shows a succession of wave profiles in the reference frame which has water at depth at rest. The paths of surface particles are indicated by dotted lines. The extra partial profile indicates the last calculations which we consider to be reliable for both particle displacements and velocities (see Sec. 3).

A good way to illustrate the velocity field of an irrotational flow is by the use of equipotentials and streamlines. Cokelet (1979) outlines how to calculate these inside the fluid from surface-evaluated quantities using Cauchy's theorem. Figure 2 shows such isolines for a full wave profile with the fluid at rest at great depth, and Figure 3 gives details near the crest at a slightly later time. These are not as informative as such diagrams for steady flows since the approach to breaking is unsteady. The fluid does not travel along fixed streamlines, but rather the flow is instantaneously tangent to changing streamlines.

Clearly it would be an improvement to consider flow in a reference frame moving with the wave crest. However there is no unique velocity that can be chosen. Any particular feature of the wave could be used to define a velocity, but that velocity would be unsteady. In Figures 4 and 5 we have chosen to view the flow of Figures 2 and 3 in a reference frame moving with the speed of the original steady wave. This gives another, possibly clearer, picture of the motion, and there are some indications that this particular reference frame is of especial relevance. This aspect is being studied further.

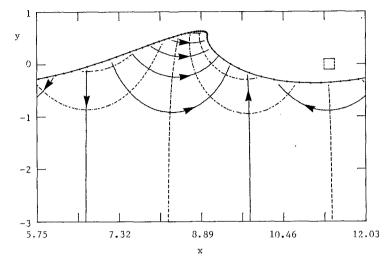


Figure 2. Equipotentials (dashed) and streamlines (solid) at  $t \approx 4.61$ for p = 0.146 in a frame of reference with water at great depth at rest. The box at upper right represents contour spacing corresponding to a dimensionless velocity of 1.

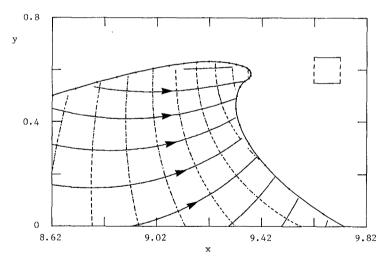


Figure 3. As for Figure 2 but near the crest at t = 4.82.

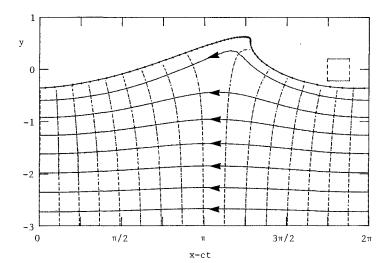


Figure 4. Equipotentials (dashed) and streamlines (solid) at t = 4.61 for p = 0.146 in a frame of reference moving with speed c =  $1^{\circ}_{\cdot}082$  relative to water at great depth.

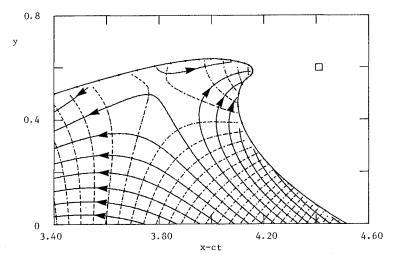


Figure 5. As for Figure 4 but near the crest at t = 4.32.

### 3. The Hodograph Plane

The search for a relevant reference frame leads to consideration of the hodograph plane. That is the (u,v) plane where u and v are, respectively, the horizontal and vertical components of velocity. A change of reference frame by a Galilean transformation (i.e. involving only a uniform constant relative velocity) corresponds only to a change of origin in the (u,v) plane. Thus the character of the (u,v) trajectory for any particle, or of the (u,v) "profile" of surface particles at any instant is unchanged. For a motion which is steady in some Galilean reference frame the trajectory of surface particles is the same as the profile of those particles at any instant. For example, it is a circle for infinitesimal waves on deep water.

To help the reader appreciate the hodograph plane in this context Figure 6 shows the surface particle trajectory/profile for the initial steady wave. The origin in this example corresponds to water at depth. Different portions of the wave are labelled. The crest-trough asymmetry is clear.

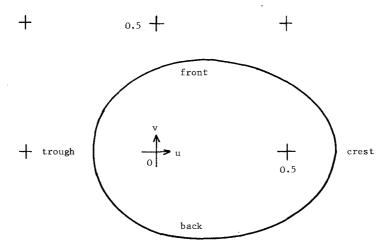


Figure 6. The hodograph plane for surface particles on a steady wave, H/L = 0.13, ak = 0.40.

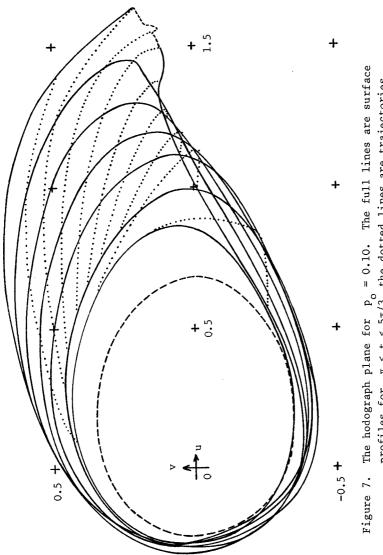
The (u,v) profiles of the surface of waves approaching breaking are shown in Figures 7 and 8 together with some of the (u,v) trajectories of surface particles.

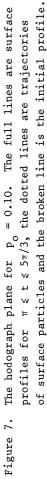
There are several features to note in these figures. Firstly each successive profile differs from its predecessor, especially on the front and crest of the wave. Secondly the magnitude of the maximum velocities continually increases. In particular the maximum horizontal velocity component soon exceeds one, the phase velocity of infinitesimal waves, and also 1.093 the maximum phase velocity of waves of this wavelength.

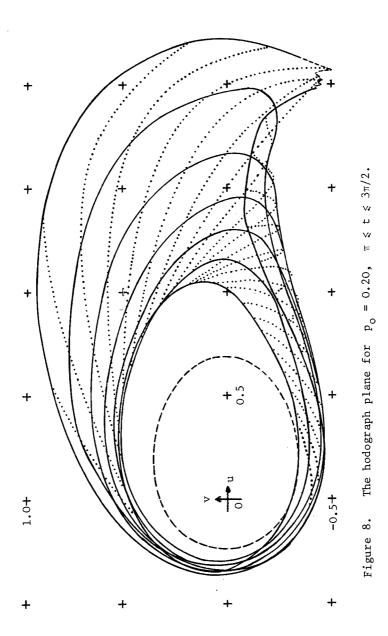
Further, the rate of increase of velocity also increases. That is, the acceleration of some particles increases. These particles are on the front of the wave. The dynamical importance of particle acceleration leads us to draw the corresponding profiles and trajectories in the acceleration plane (see the next section).

The last profile illustrated is not smooth. This indicates that the numerical method becomes inaccurate probably because the surface curvature is too great to be resolved by 60 points along the wave profile. This happens only in the region where a jet is beginning to form. Further development in time can be computed. The particle positions in the (u,v) plane, and eventually in space, become more irregular but do follow a general pattern similar to that which is to be expected for a jet. That is, particles converge towards a free fall trajectory which has a constant horizontal velocity component and a uniformly accelerating downward velocity component.

An envelope of trajectories and profiles is a prominent feature of Figure 8. It cannot be considered as typical since it does not occur in Figure 7. However, one point of that envelope is noteworthy. From the smoothness and continuity of the curves it is easy to deduce that one particle trajectory approaches the envelope and then recedes away from it without any tangential component along the envelope at the instant it touches. This is clear since some particles move to the left and some to the right. At the instant this particular particle is at the envelope it has zero acceleration. As may be seen in the next section there is nothing special about the value zero, but it is representative of a region of water of low acceleration.







### 4. The Acceleration Plane and Pressure

The hodograph plane indicates both large and small particle accelerations. It is particle accelerations that are important in dynamics and it has proved instructive to draw surface profiles and particle trajectories in the particle acceleration plane (Du/Dt, Dv/Dt). As a guide Figure 9 shows the surface profile and particle trajectories of the initial progressing wave. These are coincident as in the hodograph plane. The crest-trough asymmetry is also clear.

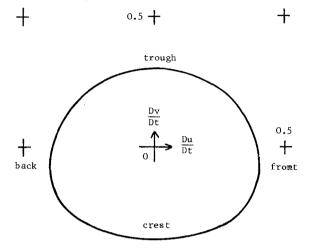
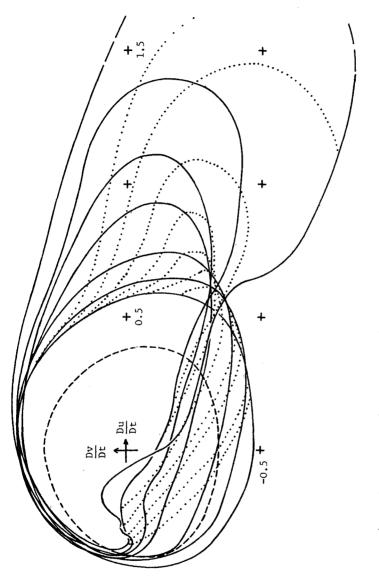


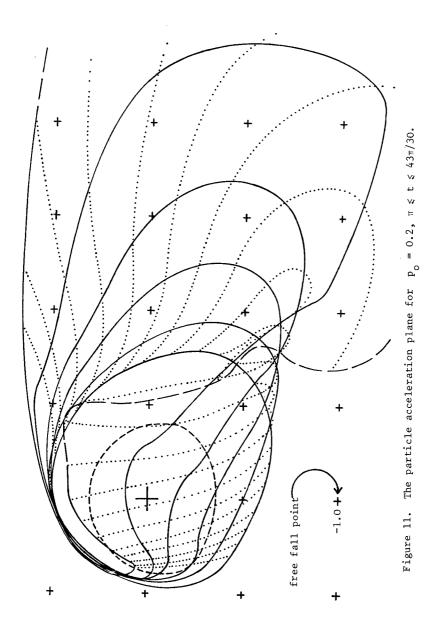
Figure 9. The particle acceleration frame for surface particles on a steady wave, H/L = 0.13, ak = 0.40.

For the approach to breaking the particle trajectories and surface profiles of acceleration show very large departures from the steadystate, as Figures 10 and 11 show. These are for the same two examples as the hodograph plane of Figures 7 and 8. The greatest reliably computed accelerations are so large, e.g. (4.3, -2.0) for Figure 11 that they have been left beyond the margins of the figures rather than reduce the scale of the more complex region illustrated.

The region of high accelerations, i.e. accelerations greater than gravity, is the dominant first impression from these figures. The region in (x,y) space which has these accelerations is the steep front portion of the wave just below the crest. In that region, water which was originally in the trough travelling towards the crest is accelerated in a relatively short time until it is travelling with or faster than the crest. It is thus not surprising that the largest component of acceleration is in a horizontal direction.







In all these cases the direction of large accelerations is such that it is directed away from the surface. This implies there is no tendency to a Rayleigh-Taylor instability which occurs if the total acceleration field is directed into the fluid. The downward accelerations which are greater than gravity are for overhanging parts of the free surface so they do not contradict this statement.

For water to receive a large acceleration there must be a corresponding large pressure gradient. At all surface points the pressure gradient is normal to the surface and directed inwards since the pressure is zero at the free surface. Figure 12 is a vector diagram of the equation of motion,

$$\rho_{\widetilde{Dt}}^{\mathrm{Du}} = -\nabla p + \rho g$$

to illustrate this.

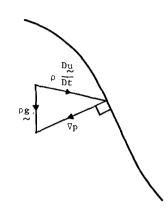


Figure 12. The equation of motion at the free surface.

The quantity  $p+\rho gy$  is a good indicator of acceleration since it is a particle-acceleration potential,

$$\rho_{\underline{i}}^{\underline{b}\underline{u}} = -\nabla(p + \rho g y).$$

Figure 13 shows a contour plot of  $p + \rho gy$  near the crest of the wave of Figures 2 and 4. The large gradients below the crest are clear. The direction of acceleration is perpendicular to the contours and is directed away from the closed contour. When the jet reaches a state of free-fall the particles must be at (0,-1) in the acceleration plane.

A region of low acceleration shows clearly at the crest and its back in Figure 13 which includes a point of zero acceleration, and the same feature is also clear in Figures 10 and 11. Figure 11 includes the zero-acceleration point passing through the surface profile but also indicates that it has no special place in the acceleration plane.

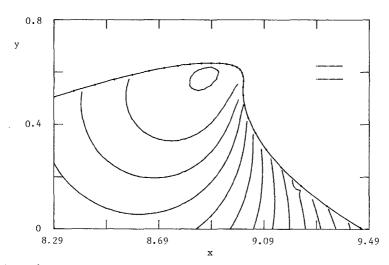


Figure 13. Lines of constant acceleration potential at t = 4.61 for p = 0.146. The pair of parallel lines at upper right indicate the spacing for an acceleration equal to that of gravity.

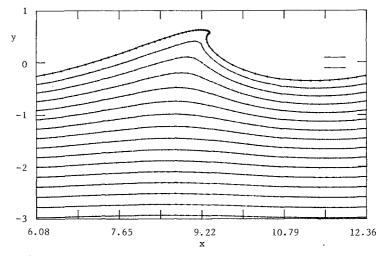


Figure 14. The pressure distribution at t = 4.82 for  $p_0 = 0.146$ .

The low acceleration region has a pressure distribution little different from hydrostatic. This particular region might be thought of as providing a "support" for the strong pressure gradient accelerating the front of the wave.

The pressure distribution for much of the flow at one time is shown in Figure 14. One aspect of it is relevant to the interpretation of pressure measurements beneath waves. The maximum of pressure at any level shows a significant variation of phase with depth. This means that the usual deductions about free-surface shape from pressure measurements are likely to be in serious error for waves at or near breaking.

# 5. Concluding Discussion

Analysis of the velocities and accelerations of a wave approaching breaking indicates three features that may be important in its dynamics. These are regions with:

- (i) a velocity greater than the maximum phase velocity for
- that wavelength,
- (ii) water particle accelerations greater than gravity,
- (iii) low particle accelerations.

All these three regions become evident well before breaking is indicated by the presence of a projecting jet. The extent of these regions at the time at which the wave face becomes vertical is indicated in Figure 15. The development of the regions in time is indicated in Figure 16.

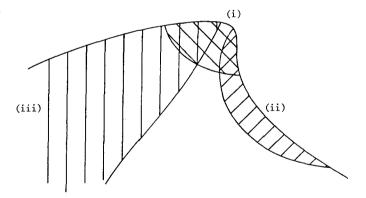
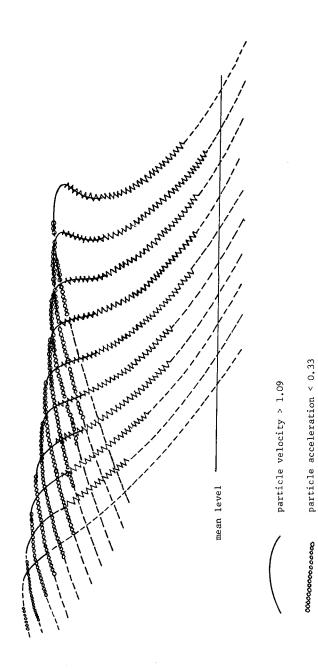


Figure 15. The crest of a wave at t = 4.61 for p = 0.146. Region (i) u > 1.09, (ii) |Du/Dt| > 1, (iii) |Du/Dt| < 0.33.







particle acceleration > 1.00

munum

Each of these regions could be defined slightly differently, and although with a given set of bounding conditions the appearance of one may precede another there is no clear indication that any one appears first. For example, for p = 0.146 at t = 3.87, the horizontal velocity has just exceeded 1.10, the maximum acceleration has reached 0.98 and the minimum acceleration is 0.30.

Some surprise has been felt at the maximum accelerations calculated, though once the flow is considered carefully they are entirely consistent. It would be interesting to have confirmation from experiments or observations of water waves, but accelerations are difficult quantities to measure in a difficult environment for instruments. A small, freely floating accelerometer may be the best direct approach to measuring them.

The influence of the high accelerations on any fixed object in the path of a breaking wave could also be important. Not only is there a drag force due to the velocity but also an inertial force due to the strong pressure gradient. In addition both these forces act in nearly the same direction, whereas for a steadily progressing wave the accelerations and velocities are more or less perpendicular to each other.

Only a few examples of waves approaching breaking have been examined in detail, and it is certain that the features described here do not occur in all breaking waves. However, for plunging breakers we have examined other examples and found reasonable agreement with the above description.

#### Acknowledgement

P. McIver acknowledges the support of the Science Research Council.

#### References

- Cokelet, E. D. (1979) Breaking waves the plunging jet and interior flow-field, <u>Mechanics of Wave-Induced Forces on Cylinders</u> (ed. T. L. Shaw), pp. 287-301. San Francisco: Pitman.
- Longuet-Higgins, M. S., and Cokelet, E. D. (1976) The deformation of steep surface waves on water I. A numerical method of computation. Proc. R. Soc. Lond. A 350, 1-26.
- Longuet-Higgins, M. S., and Cokelet, E. D. (1978) The deformation of steep surface waves on water II. Growth of normal-mode instabilities. <u>Proc. R. Soc. Lond.</u> A 364, 1-28.